Precise method to control elastic waves by conformal mapping

Yongquan Liu, Wei Liu, and Xianyue Su[a)]

LTCS and Department of Mechanics and Aerospace Engineering, College of Engineering, Peking University, Beijing 100871, China

(Received 10 October 2012; accepted 29 January 2013; published online 10 March 2013)

Abstract The transformation method to control waves has received widespread attention in electromagnetism and acoustics. However, this machinery is not directly applicable to the control of elastic waves, because it has been shown that the Navier's equation does not usually retain its form under coordinate transformation. In this letter, we prove the form invariance of the Navier's equation under the conformal mapping based on the Helmholtz decomposition method. The needed material parameters are provided to manipulate elastic waves. The validity of this approach is confirmed by an active stealth device which can disguise the signal source by changing its position. Experimental verifications and potential applications may be expected in nondestructive testing, structural seismic design and other fields. [doi:10.1063/2.1302112]

Keywords transformation method, elastic waves, conformal mapping, Helmholtz decomposition method, metamaterials

The electromagnetic (EM) wave transformation method, reported by Leonhardt[1] and Pendry et al.,[2] has recently attracted significant attention. This method is based on the form invariance of Maxwell's equations under any coordinate transformations. It offers a versatile tool to control the electromagnetic field, and many novel ground-breaking devices for electromagnetic waves and light, such as invisibility cloaks[1–5] and super lens,[6,7] are conceived based on this method. Meanwhile, the equations describing electromagnetic waves and acoustic waves have great similarities, many recipes derived for electromagnetic applications can be extended to the acoustics domain, and some types of acoustic devices could be realized using materials with specific bulk modulus and mass density.[8–11] Generally speaking, materials designed by the transformation method are highly inhomogeneous, anisotropic and even negative, which leads to that most of the existing designs just remain in the realm of an academic exercise. For easier fabrication, massive efforts have been devoted to simplifying the needed parameters of metamaterials. Some researchers have studied the effects of simplifying the material parameters to maximize the practicality of the design,[5,12,13] but these approximations often lead to significantly decreased performance. Another approach considers conformal or quasi-conformal transformations to simplifying the materials by minimizing the anisotropic and inhomogeneous parameters.[3,14]

However, the application of transformation method to elastic waves does not always work, although some elastic cloaks have been studied and designed.[15–18] Milton et al.[19] have proved that elastic waves are different from the acoustic and electromagnetic counterparts, because the form of conventional elastodynamic equation (i.e., the Navier's equation) will be transformed into the Willis equations under general coordinate transformations. Norris and Shuvalov[20] have reconsidered the variation of elastodynamic equations with the coordinate transformations, and find that the stiffness matrix in the transformed material is asymmetric unless the displacement gauge matrix is identical to the transformation matrix. Recently, Hu et al.[21–23] proposed an approximate method to guide elastic waves. They showed that the Navier's equation keeps its form under the local affine transformation, but it is true only if the frequency is high or the material gradient is small. Although the transformed parameters derived by the local affine transformation method are simpler in form and easier to achieve relatively, the practical fabrication of those newfangled devices is still an immense difficulty, because the necessary metamaterials are usually highly anisotropic, inhomogeneous and even negative.[24–27] Moreover, unlike the natural negative electric permittivity, no natural material with negative mass density or negative modulus has been found, which makes the realization of acoustic/elastic metamaterials much more challenging. Thus, practical devices made of metamaterials to control elastic waves are not yet available.

In light of this, it is reasonable to ask whether the form invariance of the elastic governing equation, i.e., the Navier's equation, establishes in conformal mapping cases. In this paper, by using the Helmholtz decomposition, we will prove that the answer is yes. The form of Navier's equation remains unchanged under conformal mapping of coordinate system. Thus the numerous conclusions derived for electromagnetic and acoustic applications can also be applied in solid mechanics, as long as in the conformal mapping range. To validate the effectiveness of the proposed approach, an active stealth device which can disguise the signal source by changing its position, is proposed based on the presented theory and numerically simulated with the finite element method. To the best of our knowledge, this device is the first one to camouflage a region with a source generating elastic waves.

[a)]Corresponding author. Email: xyswsk@pku.edu.cn.

In the homogeneous isotropic elastic solid medium, the governing equation in terms of displacement can be described by the well-known Navier's equation

$$(\lambda+\mu)\nabla(\nabla\cdot\boldsymbol{u})+\mu\nabla^2\boldsymbol{u}+\rho\boldsymbol{F}=\rho\ddot{\boldsymbol{u}}, \tag{1}$$

where $\boldsymbol{u}$ is the displacement vector, ρ is the mass density and $\boldsymbol{F}$ is the body force. The elastic constants λ and μ are known as the Lamé constants. By introducing the scalar and vector potentials $\varPhi$ and $\boldsymbol{H}$

$$\boldsymbol{u}=\nabla\varPhi+\nabla\times\boldsymbol{H},\quad \nabla\cdot\boldsymbol{H}=0, \tag{2}$$

and we also express the body force $\boldsymbol{F}$ as

$$\boldsymbol{F}=\nabla f+\nabla\times\boldsymbol{B},\quad \nabla\cdot\boldsymbol{B}=0. \tag{3}$$

where f and $\boldsymbol{B}$ are the scalar and vector potentials of $\boldsymbol{F}$, then substitute Eqs. (2) and (3) into Eq. (1), with the fact that $\nabla\cdot\nabla\varPhi=\nabla^2\varPhi$, $\nabla^2(\nabla\varPhi)=\nabla\left(\nabla^2\varPhi\right)$ and $\nabla\cdot(\nabla\times\boldsymbol{H})=0$, we have

$$\nabla[(\lambda+2\mu)\nabla^2\varPhi+\rho f-\rho\ddot{\varPhi}]+ \nabla\times(\mu\nabla^2\boldsymbol{H}+\rho\boldsymbol{B}-\rho\ddot{\boldsymbol{H}})=\boldsymbol{0}. \tag{4}$$

Equation (4) will be satisfied if each bracketed term vanishes, thus giving

$$(\lambda+2\mu)\nabla^2\varPhi+\rho f-\rho\ddot{\varPhi}=0, \tag{5}$$

$$\mu\nabla^2\boldsymbol{H}+\rho\boldsymbol{B}-\rho\ddot{\boldsymbol{H}}=\boldsymbol{0}. \tag{6}$$

The process described above is called the Helmholtz decomposition, and Eqs. (5) and (6) are the scalar and vector Helmholtz equations, respectively. It seems that values of $\varPhi$ and $\boldsymbol{H}$ not satisfying these two equations might still cause the original Eq. (1) to be satisfied. Fortunately, it has been established by Sternberg[28] that the complete solution is given by the solution of Eqs. (5) and (6). Therefore, these two Helmholtz equations are equivalent to the Navier's equation (1), we just need to consider Eqs. (5) and (6), instead of the Navier's equation.

With an $\exp(-\mathrm{i}\,\omega t)$ time dependence, Eqs. (5) and (6) can be rewritten as

$$\nabla^2\varPhi+\omega^2\frac{1}{C_{\mathrm{L}}^2}\varPhi=-\frac{1}{C_{\mathrm{L}}^2}f, \tag{7}$$

$$\nabla^2\boldsymbol{H}+\omega^2\frac{1}{C_{\mathrm{T}}^2}\boldsymbol{H}=-\frac{1}{C_{\mathrm{T}}^2}\boldsymbol{B}, \tag{8}$$

where ω is the circular frequency, $C_{\mathrm{L}}=\sqrt{(\lambda+2\mu)/\rho}$ and $C_{\mathrm{T}}=\sqrt{\mu/\rho}$ are the velocity of longitudinal wave and transverse wave, respectively.

Now we investigate the above two equations in the conformal transformation. As the conformal mapping in three dimensions is virtually nonexistent except the so-called sphere inversion transformation, we study the case of two dimensional (2D) conformal mapping in this paper. In practice, this 2D conformal mapping can be used to deal with plane strain problems in which no transformation is assumed in the off-plane direction. For the convenience of elaboration, the complex number $z=x+\mathrm{i}\,y$ as well as its partial derivatives $\partial x=\partial z+\partial z^*$ and $=\mathrm{i}\,\partial z-\mathrm{i}\,\partial z^*$ are used, where the asterisk symbolizes complex conjugation, and then we have $\nabla^2=\partial x^2+\partial y^2=4\partial z\partial z^*$. Suppose we introduce new coordinates $w=u+\mathrm{i}\,v$ described by an analytic function that does not depend on z^*. It can be easily derived that

$$\begin{aligned}\nabla^2=\frac{\partial^2}{\partial x^2}+\frac{\partial^2}{\partial y^2}=&\left[\left(\frac{\partial u}{\partial x}\right)^2+\left(\frac{\partial u}{\partial y}\right)^2\right]\frac{\partial^2}{\partial u^2}+\\ &2\left(\frac{\partial u}{\partial x}\frac{\partial v}{\partial x}+\frac{\partial u}{\partial y}\frac{\partial v}{\partial y}\right)\frac{\partial^2}{\partial u\partial v}+\\ &\left[\left(\frac{\partial v}{\partial x}\right)^2+\left(\frac{\partial v}{\partial y}\right)^2\right]\frac{\partial^2}{\partial v^2}+\\ &\left(\frac{\partial^2 u}{\partial x^2}+\frac{\partial^2 u}{\partial y^2}\right)\frac{\partial}{\partial u}+\left(\frac{\partial^2 v}{\partial x^2}+\frac{\partial^2 v}{\partial y^2}\right)\frac{\partial}{\partial v}.\end{aligned}$$

The analytic functions satisfy the Cauchy–Riemann equations

$$\frac{\partial u}{\partial x}=\frac{\partial v}{\partial y},\quad \frac{\partial v}{\partial x}=-\frac{\partial u}{\partial y}. \tag{9}$$

Then we have

$$\left(\frac{\partial u}{\partial x}\right)^2+\left(\frac{\partial u}{\partial y}\right)^2=\left(\frac{\partial v}{\partial x}\right)^2+\left(\frac{\partial v}{\partial y}\right)^2=\left|w'(z)\right|^2,$$

$$\frac{\partial u}{\partial x}\frac{\partial v}{\partial x}+\frac{\partial u}{\partial y}\frac{\partial v}{\partial y}=\frac{\partial^2 u}{\partial x^2}+\frac{\partial^2 u}{\partial y^2}=\frac{\partial^2 v}{\partial x^2}+\frac{\partial^2 v}{\partial y^2}=0.$$

Thus

$$\nabla^2=\left|w'(z)\right|^2\left(\frac{\partial^2}{\partial u^2}+\frac{\partial^2}{\partial v^2}\right)=\left|w'(z)\right|^2\nabla'^2.$$

In the new coordinate, the scalar quantities are invariant, i.e., $\varPhi'=\varPhi$ and $f'=f$. However, the vector quantities will change with the coordinate transformation, namely, $\boldsymbol{H}'=\boldsymbol{A}\cdot\boldsymbol{H}$ and $\boldsymbol{B}'=\boldsymbol{A}\cdot\boldsymbol{B}$, where $\boldsymbol{A}$ is the Jacobian matrix. Then it can be proved that $\left|w'(z)\right|^2\nabla'^2\boldsymbol{H}'=\boldsymbol{A}\cdot\left(\nabla^2\boldsymbol{H}'\right)$, if the Cauchy–Riemann equations are met, and Eqs. (7) and (8) become

$$\nabla'^2\varPhi'+\omega^2\frac{1}{C_{\mathrm{L}}'^2}\varPhi'=-\frac{1}{C_{\mathrm{L}}'^2}f', \tag{10}$$

$$\nabla'^2\boldsymbol{H}'+\omega^2\frac{1}{C_{\mathrm{T}}'^2}\boldsymbol{H}'=-\frac{1}{C_{\mathrm{T}}'^2}\boldsymbol{B}', \tag{11}$$

with

$$\frac{1}{C_{\mathrm{L}}'^2}=\frac{1}{\left|w'(z)\right|^2}\frac{1}{C_{\mathrm{L}}^2},\quad \frac{1}{C_{\mathrm{T}}'^2}=\frac{1}{\left|w'(z)\right|^2}\frac{1}{C_{\mathrm{T}}^2},$$

namely

$$\frac{\rho'}{(\lambda'+2\mu')}=\frac{1}{|w'(z)|^2}\frac{\rho}{(\lambda+2\mu)},\quad \frac{\rho'}{\mu'}=\frac{1}{|w'(z)|^2}\frac{\rho}{\mu}. \tag{12}$$

Comparing Eqs. (10) and (11) to Eqs. (7) and (8), we can see the form invariance of those two equations clearly. Thus the form of Navier's equation remains unchanged under conformal mapping, for the equivalency between Eqs. (7) and (8) with Eq. (1). Consequently, the conformal mapping method can also be applied to control elastic waves, just like the way in electromagnetism and acoustics.

When designing the devices to control elastic waves, we need to get related material parameters. Besides the constraint condition (12), we realize that the transformation region should be reflectionless with the surrounding medium, i.e., the impedance matching condition

$$\rho'(\lambda'+2\mu')=\rho(\lambda+2\mu),\quad \rho'\mu'=\rho\mu, \tag{13}$$

should be satisfied according to the impedance matching requirement. From Eqs. (12) and (13), we can get constitutive parameters of the transformation region as follows

$$\rho'=\rho/|w'(z)|,\ \lambda'=\lambda|w'(z)|,\ \mu'=\mu|w'(z)|. \tag{14}$$

In general, the parameters of isotropic elastic solids are defined with the Young's modulus $E=\mu(3\lambda+2\mu)/(\lambda+\mu)$ and the Poisson's ratio $v=\lambda/(2\lambda+2\mu)$. It can be obtained according to Eq. (14) that

$$\rho'=\rho/|w'(z)|,\quad E'=E|w'(z)|,\quad v'=v. \tag{15}$$

Equation (14) or (15) provides the material parameters to control elastic waves by conformal mapping, which are the same as the parameters derived by the local affine transformation method.[21] But in Ref. 21, it is an approximate method under the hypotheses of local affine transformation by mapping at each point, which means that the material is considered as homogeneous around a point. So it applies only when the material gradient is small or the frequency is high. However, in contrast to it, we have proved strictly the form invariance of Navier's equation under conformal mapping. The method presented here is an accurate method to control elastic waves as required. There is no additional restriction in application. Therefore, it provides theoretic foundations to design devices to control elastic waves to some extent. In addition, it is worth stressing that the quasi-conformal transformation[3,15,29] may be used to control elastic waves with isotropic materials in the three-dimensional space, which requires further investigation in future studies.

To demonstrate the validity of our approach, we propose an active stealth device and validate it through numerical simulation. A schematic representation of this device is illustrated in Fig. 1. In physical space, the object region with wave sources (i.e., the red circular area) is located in the background medium and surrounded by the active stealth device (i.e., the cloak), but the cloak can deflect the waves in a certain way. Then observers may be cheated by deeming the object region is located in another place, as if in the virtual space shown in Fig. 1. That is to say, the active stealth device can disguise the object region with wave sources by changing its position. As far as we know, this device is the first one to camouflage a certain area by controlling elastic waves.

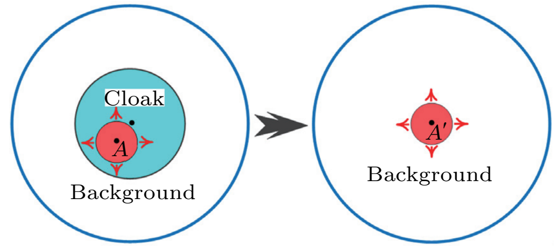

(a) The original coordinate (i.e., the physical space) (b) The transformed coordinate (i.e., the virtual space)

Fig. 1. The schematic diagram of an active stealth device.

The active stealth device can be designed by the bilinear fractional transformation (the Mobius transformation),[30] which can be expressed as

$$w(z)=\frac{z-ns}{z+ns}, \tag{16}$$

where

$$s^2=c_1^2-r_1^2,$$
$$n=1/(c_1+s+b),$$
$$c_1=(r_2^2-r_1^2-b^2)/2b.$$

The related parameters r_1, r_2 and b are shown in Fig. 2. Under this Mobius transformation, the eccentric circular ring surrounded by R_1 and R_2 is mapping into the concentric ring surrounded by R_1' and R_2', but the outer boundary does not change, as illustrated in Fig. 2.

According to Eqs. (15) and (16), the material properties of the active stealth cloak can be explicitly calculated. As an example, we set $r_1=1$ m, $r_2=5$ m and $b=3$ m, respectively. Figure 3 outlines the material properties of the device, the ratios of Young's modulus E'/E and density ρ'/ρ to the background material are plotted in Figs. 3(a) and 3(b), respectively. As can be seen from Fig. 3, another important feature of conformal mapping is that the required material properties vary within a small range. In this example, the ratio of Young's modulus and the density both range from 0.22 to 4.58.

In this simulation, we set the background material as the structural steel with elastic modulus $E=210$ GPa, density $\rho=7\,800$ kg/m^3 and Poisson's ratio

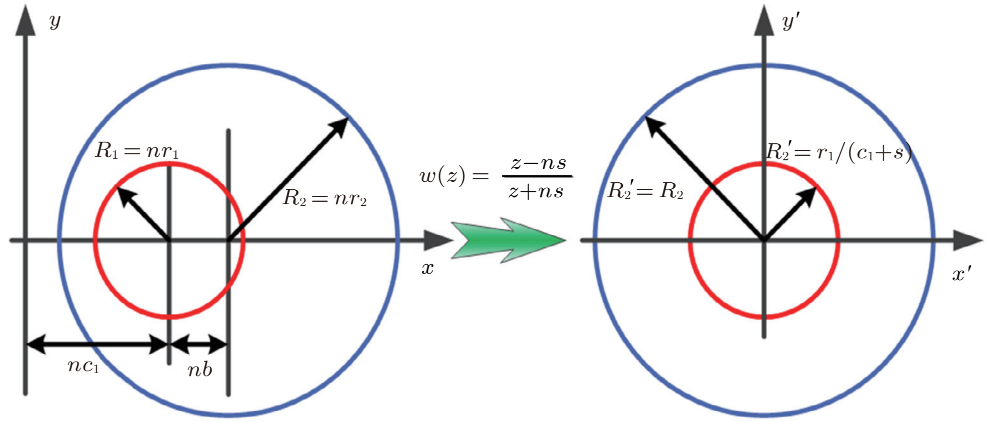

Fig. 2. The geometrical relationships of the Mobius transformation, related parameters are defined on the drawing.

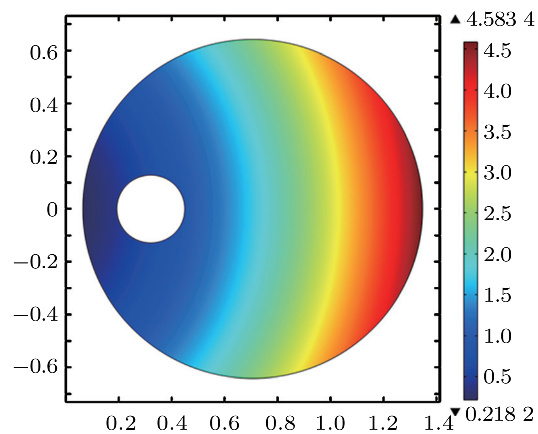

(a) The distribution of E'/E

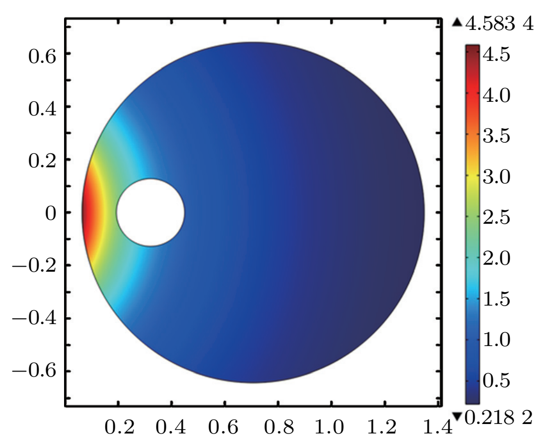

(b) The distribution of ρ'/ρ

Fig. 3. The material parameters ratio of the active stealth cloak.

$\nu = 0.3$. The perfectly matched layer (PML) is set on the boundary of the computed region to model the infinite elastic medium. To simulate the longitudinal wave emitting from the center of the objective region, a small circle of radius $r = 0.03$ m is designed, and we set its boundary as 1 m/s^2 initial radial acceleration.

Figure 4 shows the distribution of total displacement in the simulated region. To prove the validity of the conformal mapping method both at high and low frequencies, three different frequencies are considered. In Figs. 4(a)–4(c), the objective region is off-center and covered by the active stealth device, and waves are excited from the center of the object region at frequency of 10 kHz, 20 kHz and 30 kHz, respectively. To mimic the virtual space shown in Fig. 1, the cloak is removed in Figs. 4(d)–4(f), and the waves emit at the center of the simulated domain at frequency of 10 kHz, 20 kHz and 30 kHz accordingly. It can be seen that the wave profile in the background medium agrees quite well with each other, whether at high or low frequencies. This means that the designed device can disguise a region with elastic wave sources by changing its position. Consistent results can be gained as well if we let the shear wave emit from the center of the objective region.

It is worth noting that the wave patterns show slight differences between Figs. 4(a)–4(c) and Figs. 4(d)–4(f). In other words, unlike that in Figs. 4(d)–4(f), the intensity of the wave field in Figs. 4(a)–4(c) is not totally axisymmetric. In fact, the region will be inhomogeneous in the mapped coordinates, and the linear density is non-uniform in the boundary of the region accordingly. Consequently, if we set an axisymmetric wave source in the center of the objective region, the wave intensity will change with the position mildly in the outer area. The tiny differences should be attributed to the transformation relations described in Fig. 2. However, the discrepancy of wave intensity is acceptable to some extent, because the wave front is perfectly axisymmetric, as shown in Fig. 4. Above all, the camouflage effect of the active stealth device is obvious.

In summary, the form invariance of the Navier's equation under the conformal mapping is demonstrated by reducing the Navier's equation into two Helmholtz equations equivalently, and the material parameters to design devices for controlling elastic waves can be deduced by the conformal mapping method. In contrast to the local affine transformation method, the approach

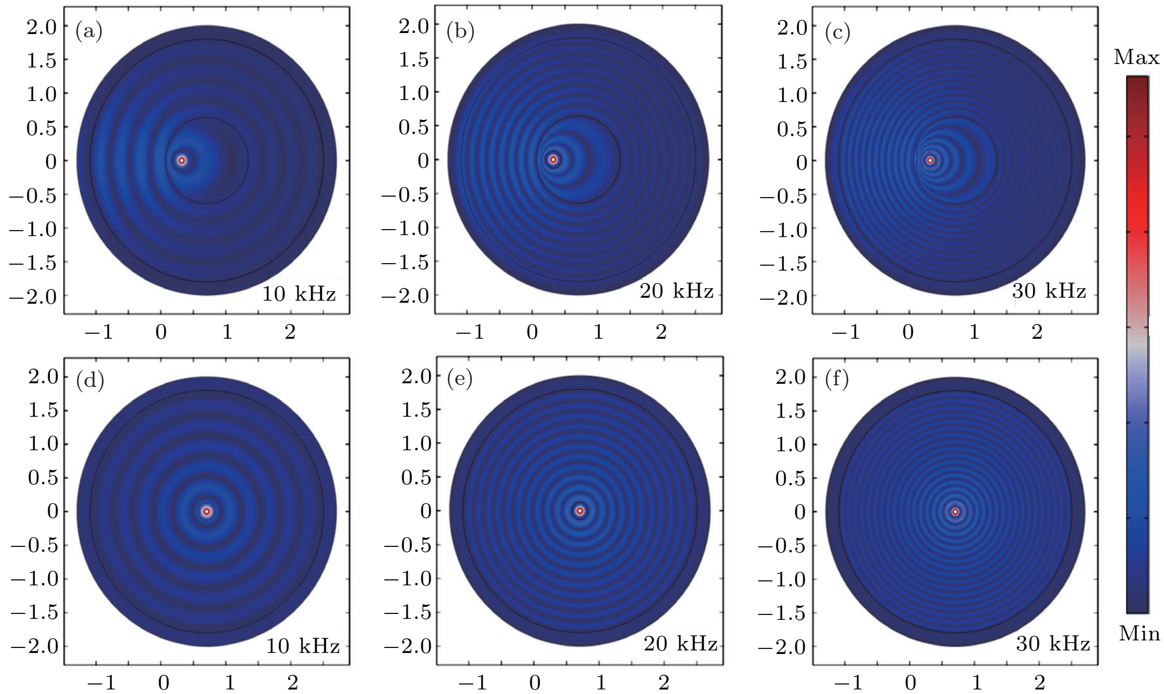

Fig. 4. The distribution of total displacement with different frequencies, the background medium is set as the structural steel. (a) The objective region is off-center and covered by the active stealth device, waves are excited from the center of the object region at frequency of 10 kHz; (b) Same to (a), but at frequency of 20 kHz; (c) Same to (a), but at frequency of 30 kHz; (d) Wave emits at the center of simulated region without the cloak at frenquency of 10 kHz; (e) Same to (d), but at frequency of 20 kHz; (f) Same to (d), but at frequency of 30 kHz.

proposed here is a precise method for controlling elastic waves, there is no additional restriction in application. Therefore, it provides theoretic foundations to design functional devices by transformation method in elastodynamics to some extent; the numerous conclusions derived in electromagnetism and acoustics can be applied in solid mechanics directly as long as in the conformal mapping range. The proposed method was demonstrated by an active stealth device which can disguise the signal source by changing its position, whether at high or low frequencies; it is the first design to camouflage a region generating waves in elastodynamics. Using the same approach, many other exciting devices could also be achieved via conformal transformation. We hope that various innovative devices can be verified experimentally, and potential applications can be anticipated in related fields.

This work was supported by the National Natural Science Foundation of China (90916007 and 91116008).

1. U. Leonhardt, Science **312**, 1777 (2006).
2. J. B. Pendry, D. Schurig, and D. R. Smith, Science **312**, 1780 (2006).
3. J. Li, and J. B. Pendry, Phys. Rev. Lett. **101**, 203901 (2008).
4. U. Leonhardt, and T. Tomáš, Science **323**, 110 (2009).
5. D. Schurig, J. J. Mock, and B. J. Justice, et al., Science **314**, 977 (2006).
6. J. B. Pendry, Phys. Rev. Lett. **85**, 3966 (2000).
7. R. A. Shelby, D. R. Smith, and S. Schultz, Science **292**, 77 (2001).
8. S. A. Cummer, and D. Schurig, New J. Phys. **9**, 45 (2007).
9. H. Y. Chen, and C. T. Chan, Appl. Phys. Lett. **91**, 183518 (2007).
10. S. A. Cummer, B. I. Popa, and D. Schurig, et al., Phys. Rev. Lett. **100**, 024301 (2008).
11. C. Y. Ren, Z. H. Xiang, and Z. Z. Cen, Appl. Phys. Lett. **97**, 044110 (2010).
12. W. Cai, U. K. Chettiar, and A. V. Kildishev, et al., Nat. Photonics **1**, 224 (2007).
13. M. Yan, Z. Ruan, and M. Qiu, Phys. Rev. Lett. **99**, 233901 (2007).
14. N.I. Landy, N. Kundtz, and D. R. Smith, Phys. Rev. Lett. **105**, 193902 (2010).
15. M. Farhat, S. Guenneau, and S. Enoch, Phys. Rev. Lett. **103**, 024301 (2009).
16. M. Farhat, S. Guenneau, and S. Enoch, et al., Phys. Rev. B **79**, 033102 (2009).
17. M. Brun, S. Guenneau, and A. B. Movchan, Appl. Phys. Lett. **94**, 061903 (2009).
18. N. Stenger, M. Wilhelm, and M. Wegener, Phys. Rev. Lett. **108**, 014301 (2012).
19. G. W. Milton, M. Briane, and J. R. Willis, New J. Phys. **8**, 248 (2006).
20. A. N. Norris, and A. L. Shuvalov, Wave Motion **48**, 525 (2011).
21. Z. Chang, J. Hu, and G. K. Hu, et al., Appl. Phys. Lett. **98**, 121904 (2011).
22. J. Hu, Z. Chang, and G. K. Hu, Phys. Rev. B **84**, 201101 (2011).
23. X. M. Zhou, X. N. Liu, and G. K. Hu, Theor. Appl. Mech. Lett. **4**, 041001 (2012)

24. G. W. Milton, and J. R. Willis, Proc. R. Soc. A. **463**, 855 (2007).
25. V. Fokin, M. Ambati, and C. Sun, et al., Phys. Rev. B **76**, 144302 (2007).
26. H. H. Huang, C. T. Sun, and G. L. Huang, Int. J. Eng. Sci. **47**, 610 (2009).
27. Y. Wu, Y. Lai, and Z. Q. Zhang, Phys. Rev. Lett. **107**, 105506 (2011).
28. E. Sternberg, Archs Ration Mech. Analysis **6**, 34 (1960).
29. Y. Urzhumov, N. Landy, and D. R. Smith, J. Appl. Phys. **111**, 053105 (2012).
30. R. Schinzinger, and P. Laura, *Conformal Mapping: Methods and Applications* (Dover, New York, 2003).